Polymer Testing 117 (2023) 107837

Contents lists available at ScienceDirect

Polymer Testing

journal homepage: www.elsevier.com/locate/polytest

Measuring and mathematical modeling of cushion curves for polymeric foams

Márton Tomin [a], Márton Áron Lengyel [a], Richárd Dominik Párizs [a], Ákos Kmetty [a,b,*]

[a] Department of Polymer Engineering, Faculty of Mechanical Engineering, Budapest University of Technology and Economics, Műegyetem rkp. 3, H-1111, Budapest, Hungary

[b] ELKH–BME Research Group for Composite Science and Technology, Műegyetem rkp. 3, H-1111, Budapest, Hungary

ARTICLE INFO

Keywords:
Polymer foams
Cushion curve
Impact test
Burgess method
Mechanical characterization
Mathematical analysis

ABSTRACT

In this paper, we created a general mathematical equation for the cushion curves of polymeric foams, using the measurement results of drop weight impact tests on commercially available, closed-cell ethylene-vinyl acetate and cross-linked polyethylene foams of different densities. We found exponential relationship between the results of the drop tests and the static load, and investigated the effect of the input parameters on the fitted constants using analysis of covariance and multiple linear regression. In the second part of the study, we used a novel approach to theoretically determine the cushion curves of different thicknesses. We predicted material behavior using the Burgess method on the fitted exponential equations and assessed the limitations and accuracy of this extrapolation approach by comparing the measured and simulated data. We validated the results by quantifying the permanently damaged volume of the foams with the use of a 3D optical measuring system.

1. Introduction

During transportation and handling, consumer goods (e.g. technological products) are often subjected to impacts and shocks, which can damage them mechanically and cause permanent damage. Therefore, foamed polymer packaging materials are used to protect them and decrease the risk of mechanical damage [1]. These materials are light, so their transport causes reduced environmental pollution. Stricter and stricter environmental directives are forcing the industry to improve constantly, therefore biomaterials receive a great deal of attention, because they have a smaller ecological footprint [2]. In addition, this footprint can also be reduced if less material is used, which can achieved through accurate product design. Therefore, another important research goal is to reduce the weight of products, so foams are widely used and tested. In addition, due to their cellular structure, foams can absorb a huge amount of impact energy, while keeping the maximum acceleration acting on the product under a certain limit [3–6].

In the packaging industry, the foams used to protect the product are selected with the use of the so-called cushion curves, which are attached to the data sheet of the packaging material. These curves summarize the maximum absolute acceleration (marked with G in Fig. 1.) results of several drop-weight tests as a function of static load and are available for several drop heights. The static load is the compressive stress to which the foam under the product is subjected during storage (1).

$$s = \frac{mg}{A}\ [\mathrm{Pa}] \tag{1}$$

where s [Pa] is the static load, m [kg] is the mass of the product, $g = 9.81$ [ms^{-2}] is gravitational acceleration, while A [m^2] is the contact area between the foam and the product [7–9].

In general, a huge number of drop tests are required to determine the cushion curve, in which the mass of the body dropped down onto the foam is continuously increased, causing the foam to give a different material response (Fig. 1).

In case of dropping down a lower weight (see m_1 in Fig. 1.), the cell structure of the foam is only minimally deformed, resulting in short impact time and, therefore, high peak acceleration (G_1). With increasing the impactor mass (m_2), the foam becomes gradually more and more deformed, and the maximum acceleration value decreases steadily until the minimum point of the cushioning curve. At the minimum point, the load (see m_2) compresses the foam until the end of the so called plateau zone [4] providing a longer path to reduce the impactor's speed without causing irreversible structural deformation. After this point, the maximum acceleration value increases again (e.g. see G_3) because the

* Corresponding author. Department of Polymer Engineering, Faculty of Mechanical Engineering, Budapest University of Technology and Economics, Műegyetem rkp. 3, H-1111, Budapest, Hungary.
E-mail address: kmetty@pt.bme.hu (Á. Kmetty).

https://doi.org/10.1016/j.polymertesting.2022.107837
Received 29 July 2022; Received in revised form 30 August 2022; Accepted 14 October 2022
Available online 20 October 2022

third zone of the stress–deformation curve (densification) [4] is reached. Here the cells are completely compacted before the impactor's speed is reduced to zero, which results in a higher peak acceleration. The shock-absorbing performance of the foam is the best in the minimum point (G_1), where the degree of deformation is optimal to absorb the impact energy and protecting the product from high peak forces [4, 7–10].

In packaging, the sensitivity of different products to mechanical load is characterized by the fragility factor, which shows the linear acceleration limit beyond which the product suffers mechanical damage. With this limit, a horizontal line can be drawn on the cushion curves to indicate critical absolute acceleration, from which the acceptable static load range can be determined where the material will absorb the impact energy and protect the product (see Fig. 2). Then the minimum required contact area can be calculated based on the mass of the product (see Equation (1)). Thus, using cushion curves is an effective way to design suitable protective packaging for a product with known requirements [7,10].

It is also important to note that besides packaging, the curves can also be used in any other areas (e.g. the sports [11] or automotive industry [12]), which exploit the advanced energy-absorbing capability of foams. In addition to their practical use, the curves illustrate the effect of impact energy (mass and drop height) and foam thickness on shock absorption, so their analysis is also important from a scientific point of view.

Despite the scientific and practical importance of the topic, most studies in the literature [13–15] and industrial applications [16,17] fit the measurement results with a polynomial equation of many degrees. These, apart from having limited physical content, only give accurate results within the measurement range and the extrapolation to higher static loads results in impossible material behavior.

Another problem is the large number of measurements needed to determine the curves. The ASTM D-1596 standard is the most commonly used test method, which defines five drops on each sample with a minimum relaxation time of 1 min between each drop. It evaluates the results of the 1st and 2nd–5th drops separately [18]. Therefore, to determine a full range of cushion curves (7 drop heights, 6 thicknesses), a minimum number of 10500 drops is necessary [1]. Thus, several theories have been published that aim to simplify the measurement process and reduce laboratory time.

Conversion from a quasi-static compression chart is the simplest way of cushion curve generation. However, studies [19,20] using this method had limited accuracy, with a difference between the measured and calculated data of at least 30%. Ramon and Miltz [21] showed that this method is only applicable to rate-independent foams, where the mechanical characteristics are not affected by the strain rate.

Thus, extrapolating methods [22–24], which calculate the curves from the results of a small series of drop tests, are more commonly used

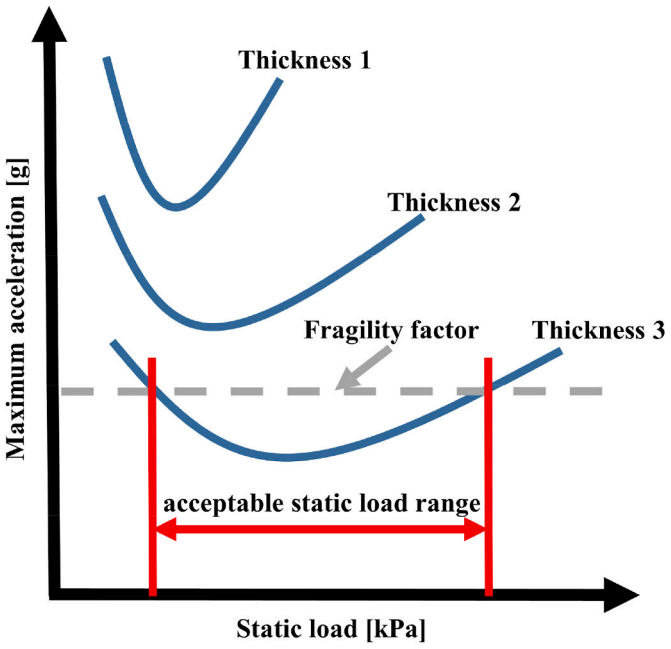

Fig. 2. Determining of the acceptable static load range with cushion curves.

to predict the cushioning behavior of packaging materials. The most widely used of these is the "equation-fitting" method published by Gary Burgess [23], which can be used to estimate the curves with high accuracy for any height and thickness from a single experimental cushion curve. The method uses the relationship between the energy density (energy absorbed per unit volume) and maximum dynamic compression stress (see Equation (2)) to predict the curves, as both parameters can be related to the cushion strain at peak compression:

$$(G+1)s \sim s\,h/t \tag{2}$$

where G is peak acceleration [g = 9,81 m/s^2], s [Pa] is the static load, h [m] is the drop height, and t [m] is the thickness of the sample. The method was validated on 32 kg/m^3 density macrocell polyethylene and 24 kg/m^3 density expanded polystyrene foams [23]. However, its accuracy on microcell foams has not been demonstrated yet, and the static load range of its applicability is also unknown. Another important but not yet investigated factor is the dependence of cushion curves on foam density. Similar to the study of Burgess [23], all of the previously published articles regarding the topic focused on decreasing testing time and defining the relationship only between drop height, thickness, and peak acceleration.

In this study, our goal was to create a general mathematical equation

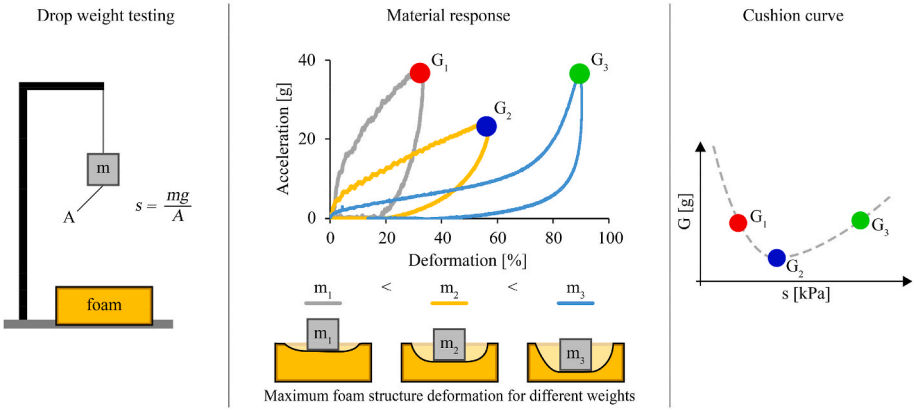

Fig. 1. Schematics of the process for determining cushion curves.

Table 1
Main characteristics of the investigated samples.

Sample name	Material	Density [kg/m^3]	Average cell size [μm]	Average cell wall thickness [μm]	Cell density [pcs/cm^3]	Investigated thickness [mm]
EVA50	EVA	50.66 ± 0.47	62 ± 26	1.2 ± 0.5	1779323	40 and 50
EVA100	EVA	96.07 ± 0.52	63 ± 22	2.4 ± 0.8	1711328	40 and 50
EVA130	EVA	130.30 ± 1.22	63 ± 29	3.3 ± 1.5	1745215	40 and 50
EVA150	EVA	147.77 ± 1.57	62 ± 28	3.7 ± 1.6	1917934	40 and 50
XPE030	XPE	28.36 ± 0.42	622 ± 151	6.7 ± 1.6	2815	40 and 50
XPE040	XPE	44.45 ± 0.36	567 ± 163	8.7 ± 2.5	4194	40 and 50
XPE050	XPE	45.70 ± 0.29	500 ± 138	9.1 ± 2.5	4839	40 and 50
XPE070	XPE	69.72 ± 0.38	464 ± 108	12.3 ± 2.9	6947	40 and 50

for the cushion curves of polymeric foams, which can be extended outside the tested static load range and include the effect of foam density. We found an exponential relationship between the results of the drop tests and the static load, and investigated the dependence of the fitted constants on the input parameters using covariance analysis and a two-factor design of experiment study. We also analyzed the accuracy and applicability of the Burgess-method [23] by comparing experimental and theoretical data.

2. Materials

The tests were carried out on commercially available ethylene-vinyl acetate (EVA) and cross-linked polyethylene (XPE) foams of different densities. The EVA foams were provided by UFM Bt. (Mosonmagyaróvár, Hungary), while the XPE foams were supplied by Polifoam Ltd. (Budapest, Hungary). The density and thickness of the foam sheets were selected based on Tomin and Kmetty [25] to cover the characteristics of foams used in the industry. Table 1 contains the labeling, density and structural properties of the tested samples.

The cell structure characteristics of the samples were determined from scanning electron microscopic (SEM) images (Fig. 3) taken with a Jeol JSM 6380LA microscope according to the method described in our previous papers [26,27].

As the images show, both foam types have a closed-cell structure, but there is an order of magnitude difference in cell size and cell density.

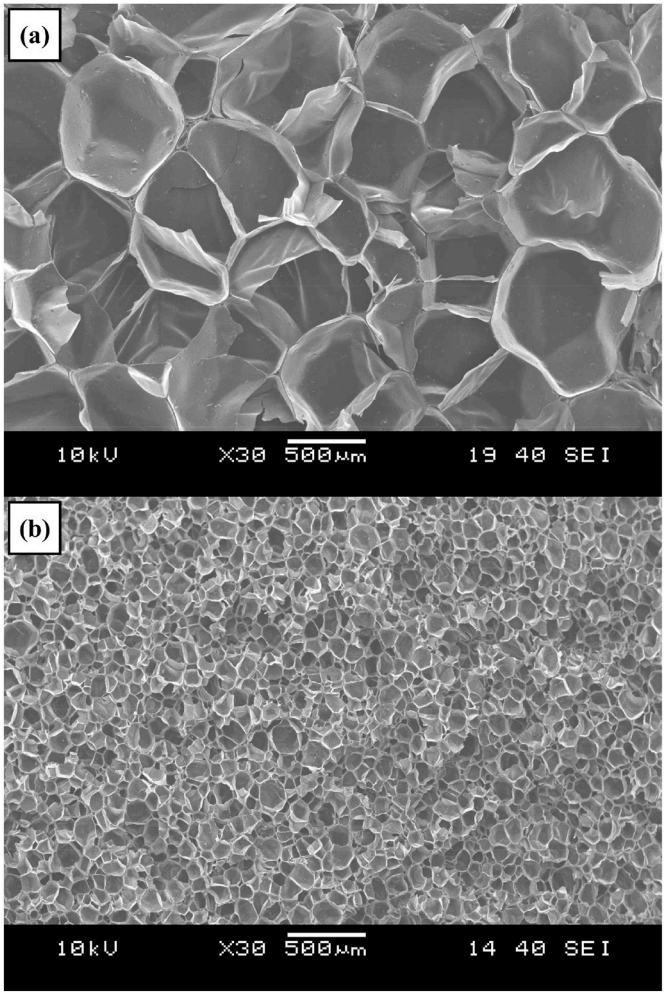

Fig. 3. SEM image of the XPE050 (a) and EVA50 (b) samples.

3. Experimental

3.1. Determining the cushion curves

3.1.1. Impact tests

In order to obtain the cushion curves of the foams, we performed drop tests using a Ceast Fractovis 9350 impact tester. The machine had a flat-end cylindrical impactor with a 50 mm diameter. The 100x100x50 mm foam specimens were placed on a 40 mm thick steel plate, which functioned as a rigid support. Five drops were performed on each specimen, and the results obtained from the 1st, and the 2nd–5th drops were treated separately in the evaluation. We waited at least 60 s between two successive drops, and executed the tests following the recommendations of ASTM D1596-97 standard. For each cushion curve, we measured at least nine points with different static load values in the range of 12–252 kPa. All measurement series were carried out at three different drop heights (200, 400 and 600 mm).

3.1.2. Mathematical modeling

The equation describing the cushion curves was determined from the relationship between the directly recorded maximum force and the static load as follows:

Since we found an exponential relationship between the two properties (see Fig. 3), first we determined the relationship between the static load and the maximum force (3), based on the measured points:

$$F_{max} = c_1 \bullet e^{c_2 s}\ [N] \tag{3}$$

where C_1 [N] and C_2 [1/kPa] are material- and drop height–dependent constants, s [kPa] is the static load and F_{max} [N] is the maximum force. Then, we calculated the dropped mass m [kg] as a function of the static load (4):

$$m = s \bullet \frac{A}{g} \bullet 1000\ [kg] \tag{4}$$

where A [m^2] is the contact area between the impactor head and the foam, s [kPa] is the static load, and $g = 9.81\ [m/s^2]$ is gravitational acceleration.

From this, the general equation of the cushion curves (5) can be written based on Newton's second law and Equations (3) and (4):

$$a = \frac{F_{max}}{m} = \frac{c_1 \bullet e^{c_2 s}}{s \bullet \mathrm{A} \bullet 1000/\mathrm{g}}\ \left[m / s^2\right] \tag{5}$$

which, after rearranging and converting to the unit of [g = 9.81 m/s^2] can be written as follows:

$$a = \frac{1}{1000 \bullet A} \bullet c_1 \bullet \frac{e^{c_2 s}}{s} \; [g] \tag{6}$$

We determined equation (6) for both materials for four different densities and three different drop heights to investigate the dependence of constants C_1 and C_2 on the input parameters.

Thus, the effect of foam density and drop height on the values of the constants was analyzed with multiple linear regression and covariance analysis. The distances between density levels were not equal for practical reasons, and one approach is to look at the levels as quantitative variables. However, they can be considered different material structures, as density is an average value with which we try to capture the characteristics of the samples. Therefore, our analysis covers both approaches with a significance level of 5%.

3.2. Predicting the cushion curve for unknown foam thicknesses

3.2.1. Drop tests and theoretical prediction

The second part of the study investigated the limitations of the Burgess approach. First, we predicted the curves of 40 mm thick foams, then checked the accuracy of prediction with performing drop tests on these samples from a drop height of 400 mm in the static load range of 12–102 kPa.

Burgess' method [23] uses linear interpolation for the estimation between the *sh/t* and *(G+1)s* auxiliary data, which does not take into account the actual shape of the cushion curves between the static load points associated with the data. However, the results are more accurate if the fitted exponential equations (see Equation (6)) are used instead of the exact measurement points.

According to the basic principle of the method (Equation (2)), the following relationships between the available and the desired data pairs can be written:

$$\frac{s_1 \bullet h_1}{t_1} = \frac{s_2 \bullet h_2}{t_2} \tag{7}$$

$$(G_1 + 1)s_1 = (G_2 + 1)s_2 \tag{8}$$

where index *1* refers to the available, while index *2* to refers to the desired data. If Equations (6)–(8) are combined after insertions and rearrangements, the estimated cushion curve can be given as:

$$G_2 = \frac{\frac{1}{1000 \bullet A} \bullet c_1 \bullet e^{\delta \bullet c_2 \bullet s_2} + \delta \bullet s_2}{s_2} - 1 \; [g] \tag{9}$$

where δ [−] is a constant that varies as a function of the available and searched thicknesses and drop heights:

$$\delta = \frac{h_2 \bullet t_1}{t_2 \bullet h_1} \tag{10}$$

With this estimation method, we predicted the curves for a drop height of 400 mm and a foam thickness of 40 mm in each case, calculating from the points of the fitted exponential equations of cushion curves of 200, 400, and 600 mm drop heights.

3.2.2. Investigating the magnitude of irreversible deformation

During the drop tests, the test specimens were damaged in several cases by the repetitive loading, and the area in contact with the impactor was torn out of the foam surface. Since the extent of damage varied visibly between foam types for the same measurement parameters, we aimed to quantify the permanently deformed volume. For this purpose, we 3D scanned the samples before and after the drop-weight test at a

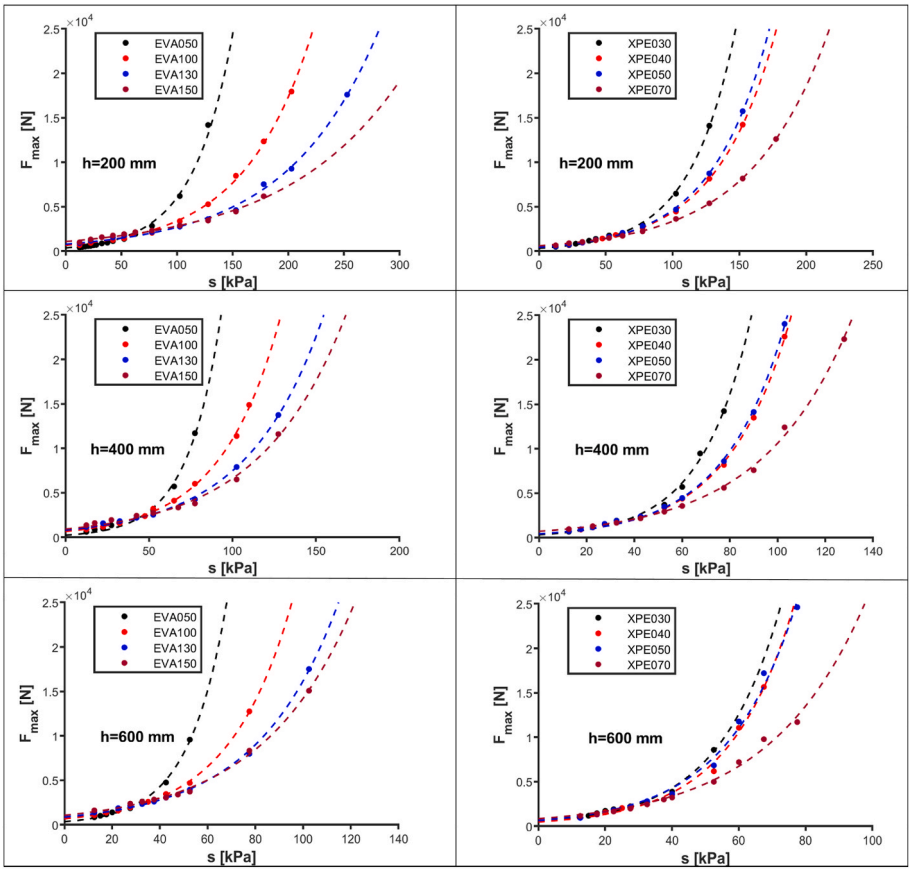

Fig. 4. Maximum force-static load diagrams for all foam types in case of different drop heights (200, 400 and 600 mm).

static load of 103 kPa using a GOM ATOS Core 5M (Gesellschaft für Optische Messtechnik GmbH, Braunschweig, Germany) optical measuring system, and determined the permanently deformed volume. Under this static load, all types of foam samples had already undergone some degree of irreversible deformation, so the differences between their materials response can be clearly illustrated.

4. Results and discussion

The results of the study can be divided into two main parts. First, we performed several drop tests to obtain cushion curves and determine a general mathematical equation that accurately describes the response of the material. Then we investigated the applicability and the limitations of using Burgess' method for cushion curve prediction.

In both cases, considering practical reasons (polymer foam products in industrial applications are subjected to repetitive impacts), the evaluation procedure is presented using the impact test results of the 2nd–5th drops.

4.1. Determining the cushion curves

4.1.1. Test results and parameter fitting

Knowing the C_1 and C_2 constants, we can determine the materials' cushion curve for any chosen drop height and foam density using equation (6). The C_i values were obtained by fitting an exponential curve to the maximum force points plotted as a function of static load, as shown in Fig. 4.

Fig. 5 shows the cushion curves fitted to the results of the drop tests. The fitted equations follow the measurement points with high accuracy for all foam types.

All the curves have the typical U shape and, in contrast to the high-order polynomial fittings [13–17], can be extrapolated outside the measured static load range, correctly describing the expected material response. The U shape can be explained with the different degrees of deformation due to the change in impact energy (see further explanation above in section 1).

4.1.2. Analyzing the effect of input parameters (foam density and drop height)

In order to design a package that provides adequate protection for a given product, one has to understand the dependence of the C_i constants on the input parameters in Equation (6). C_1 constant mainly affects the peak force and thus peak acceleration, so its increase shifts the curves upwards. Therefore, a higher C_1 value means lower protection regardless of the static load. In contrast, increasing C_2 shifts the curves to the left and upwards, which means that the foam with a lower value provides adequate protection over a wider range of static loads. In the following, the dependencies of these constants are analyzed in depth with two different approaches.

4.1.2.1. Analysis of covariance. First, we considered density as a qualitative variable and test height as a quantitative variable and applied analysis of covariance (ANCOVA) on the coefficients from the earlier regression (C_1 and C_2 in Equation (6)) separately. Then, we considered these coefficients as independent variables. The ANCOVA fits the following model (11).

$$C_k(h,j) = (\mu + \mu_j) + (\beta + \beta_j) \bullet h + \varepsilon \tag{11}$$

where C_k is the kth coefficient on the jth level of density, and with h height, μ is the grand mean, μ_j is the difference between the grand mean and the mean on the jth level of density, β is the slope fitted on the whole dataset, β_j is the difference between the jth individual slope and β, h is the measurement height and ε is the error.

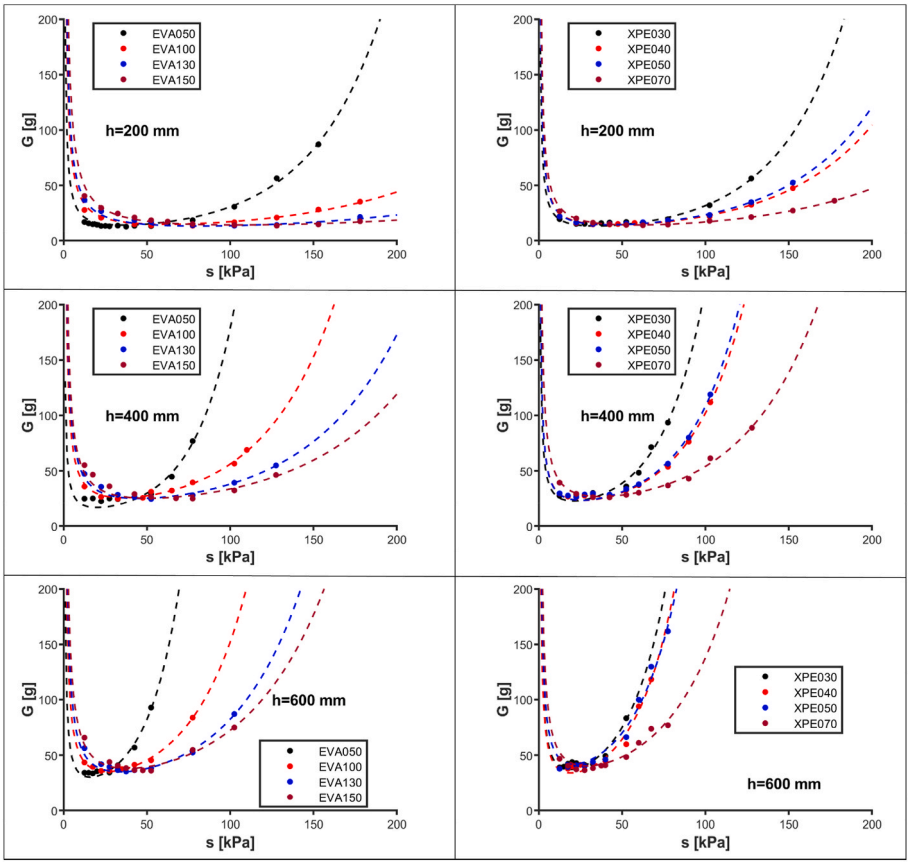

Fig. 5. Comparison of the test results and the fitted cushion curves for all foam types for different drop heights (200, 400 and 600 mm).

Table 2
Models extracted from ANCOVA.

EVA	XPE
$C_1 = (702.85 + \mu_j) + \varepsilon$ $\mu_j = \{-382.18; -36.10; 123.41; 294.88\}$	$C_1 = (373.52 + \mu_j) + 0.37 \bullet h + \varepsilon$ $\mu_j = \{-129.97; -57.29; -12.55; 199.81\}$
$C_2 = (0.0062 + \mu_j) + (5.6 \bullet 10^{-5} + \beta_j) \bullet h + \varepsilon$ $\mu_j = \{0.0057; -0.00037; -0.002; -0.0033\}$ $\beta_j = \{3.1; -0.17; -1.3; -1.6\} \bullet 10^{-5}$	$C_2 = (0.012 + \mu_j) + 5.9 \bullet 10^{-5} \bullet h + \varepsilon$ $\mu_j = \{0.0078; 0.0014; 0.0006; -0.0097\}$

From equation (11), five different relationships can be modeled. The simplest case is when each group of density can be modeled as one (which means there is no significant difference between them), and the covariate (height) does not affect the response variable (C_k). In this case $\mu_j = \beta = \beta_j = 0$ for all j's. Another possibility is that there is a significant difference between material structures, but the effect of covariate is not substantial, i.e. $\beta = \beta_j = 0$ for all j's. Only one line (with zero steepness) could describe the connection between the response and the variables in the former case. The latter model would have as many parallel lines as the number of different material structures we have. If the covariate has a significant effect on the cushion curve coefficient but there is no difference between the material structures, we would have one line again, but the slope would not be zero, i. e. $\mu_j = \beta_j = 0$ for all j's. If both material structure and drop height have a significant effect, but the latter does not depend on material structure, then parallel lines of equal (non-zero) slope model the constant, i. e. $\beta_j = 0$ for all j. In the last case, when both material structure and height have a significant effect, and the latter depends on material structure, we have different lines from which at least one is not parallel with the others, and at least one intercept is different.

We analyzed the data for each material and cushion curve coefficient to check which parameters of equation (11) are significant and how these coefficients depend on the variables. The results of the ANCOVA can be seen in Table 2.

The results show that the coefficients of the two materials can be modeled differently. It is clear from each model that changes in the structure of the materials have a significant effect on both coefficients. For EVA, the C_1 coefficient does not depend on measurement height. However, the C_2 coefficient has a slope, and the steepness of the slope depends on the structure of the foam. For XPE, both coefficients depend on measurement height, but there is no significant difference between the slopes (Fig. 6).

4.1.2.2. Multiple linear regression. The 3x4 design of this experiment allows us to use a model to describe the main effects, interactions, and higher-order effects of the test parameters. For example, the coefficients of the cushion curve could be written with a complicated polynomial relationship:

$$C_k(h,\rho) = \alpha + \beta_{1,0} \bullet h + \beta_{0,1} \bullet \rho + \beta_{1,1} \bullet h \bullet \rho + \beta_{2,0} \bullet h^2 + \beta_{0,2} \bullet \rho^2 + \ldots + \varepsilon \quad (12)$$

where C_k is the kth coefficient of the cushion curve, α is the intercept, $\beta_{i,j}$ are the model parameters where i and j show the power of height and density, respectively, h is the measurement height, ρ is the measured density of the foam, and ε is the error.

Several different static loads must be applied with repeated impact tests for a single cushion curve. Therefore, our experiment does not include replicates, in which case there will be no error term for the analysis of fitting. Usually, the second and higher-order terms (and interactions) can generally be left out of the model in practical engineering. A general linear F-test was used to ensure that this assumption was correct. The F-test compares two models, one called the "full" model and one called the "reduced" model. The statistic is based on the error of each model and the degree of freedom of the models (13).

$$F_{(df_{red}-df_{full}),df_{full}} = \frac{(SSE_{red} - SSE_{full})/(df_{red} - df_{full})}{SSE_{full}/df_{full}} \quad (13)$$

where F is the F-statistic, df_{full} is the degree of freedom of the full model, df_{red} is the degree of freedom of the reduced model, SSE_{full} is the sum of the squared errors of the full model, and SSE_{red} is the sum of the squared errors of the reduced model. The test's null hypothesis is that a phenomenon can be described by the reduced model instead of the full model. This approach can be used to check complex conditions, such as whether all third-degree terms are negligible.

This test was used to compare the full model with the reduced model, which in this case, consisted only of first-order terms without interaction terms (14). In each case, a simpler model proved more useful; in some cases, even more terms could be left out (see Table 3).

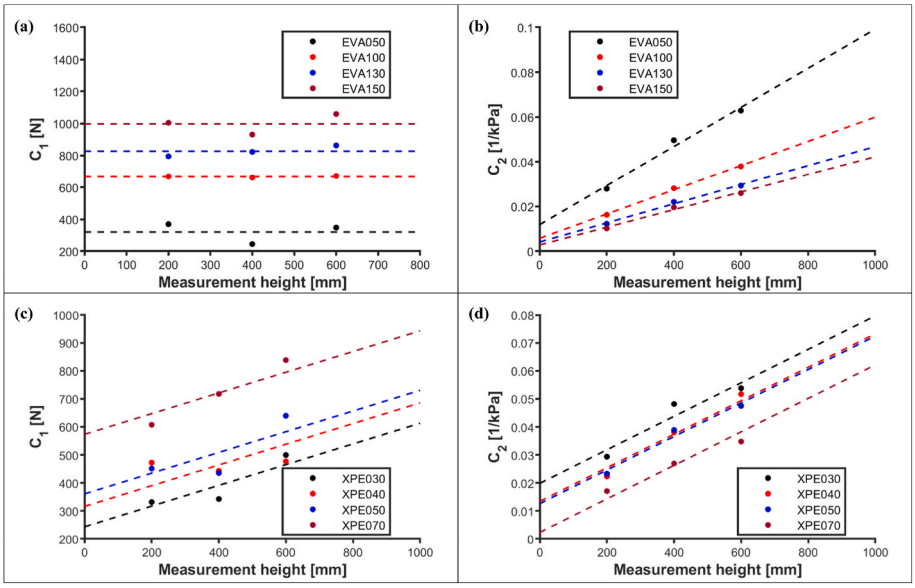

Fig. 6. Models of coefficients C_1 (a) and C_2 (b) for EVA; models of C 1 (c) and C_2 (d) coefficients for XPE.

Table 3
Linear models of the coefficients of cushion curves.

EVA	XPE
$C_1 = 6.63 \bullet \rho + \varepsilon$	$C_1 = 0.32 \bullet h + 8.2 \bullet \rho + \varepsilon$
$C_2 = 0.037 + 5.6 \bullet 10^{-5} \bullet h - 2.9 \bullet 10^{-4} \bullet \rho + \varepsilon$	$C_2 = 0.033 + 6.3 \bullet 10^{-5} \bullet h - 4.5 \bullet 10^{-4} \bullet \rho + \varepsilon$

$$C_k(h,\rho) = \alpha + \beta_1 \bullet h + \beta_2 \bullet \rho + \varepsilon \quad (14)$$

After fitting the reduced model (14), if the t-statistic of parameters showed more than one non-significant parameter, we used the general linear F-test to check the compound hypothesis. Table 3 shows the result for each material and cushion curve coefficient.

It is clear that the C_1 coefficient of EVA only depends on the density of the foam, and the effect of measurement height is negligible (see Fig. 7). Both approaches showed this phenomenon. In contrast, the C_1 coefficient of XPE depends on both measurement height and foam density.

The differences between the C_1 coefficients of the two foam types can be explained with their different material response. Generally, a higher C_1 value means higher reaction force regardless of the magnitude of the static load. As microcellular foams are more resistant to loads [28–30], we assume that the stress–strain response of the EVA foams in the investigated impact energy range varies in the plateau region, so only slight differences appear in the peak force when drop height is modified. In contrast, the impact response of the XPE foams reached the densification zone [4], which explains the significant changes in the reaction force when drop height was increased.

The results of both modeling types were determined by averaging from the 2nd–5th drops as stated in the ASTM D1596-97 standard. However, it is possible that the foam's cell structure deformed irreversibly even after the first drop. This phenomenon could result in a worse fitting and a significant change in the cushion curve coefficients. Therefore we also investigated the fitting coefficients from the 1st measurement, where both analyses gave the same type of results for each material.

4.2. Predicting the cushion curve for unknown foam thicknesses

Following the determination of the cushion curves for the 40 mm foam thicknesses, the experimental data were compared with the curves calculated from the curves of the 50 mm thick foams with the method described in Section 3.2.1. Prediction was obtained from the cushion curves for all three drop heights, the results of which, in comparison with the measured data, are shown for XPE030 and EVA150 samples in Fig. 8.

XPE030 had the worst, while EVA150 had the best match between the measured and calculated data. The accuracy of prediction for the other samples fell between these two. In the first half of the curves, the calculated and measured points run together regardless of the drop height data used for the calculation. However, above a given static load, the calculation is inaccurate and the difference between the measured and calculated values increases steadily. Calculation with a higher drop height series further increases this deviation. This tendency can be related to the degree of irreversible deformation, as the calculation can only follow the measured data up to the static load value, where permanent deformation occurs in the material structure. Above this limit, the curves determined from measurements at 200 mm, 400 mm, and 600 mm drop heights differ because increasing the impact velocity also increases the damage, thus reducing the accuracy of the calculation. It

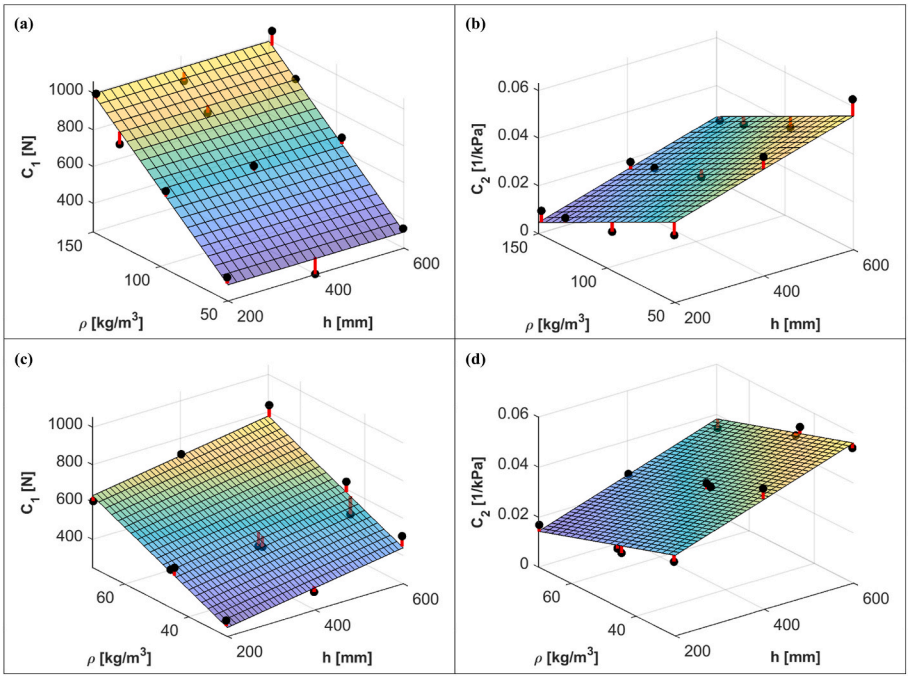

Fig. 7. Multiple linear regression of the C_1 (a) and C_2 (b) coefficients for EVA; the multiple linear regression of the C_1 (c) and C_2 (d) coefficients for XPE, residuals illustrated with red lines. (For interpretation of the references to colour in this figure legend, the reader is referred to the Web version of this article.)

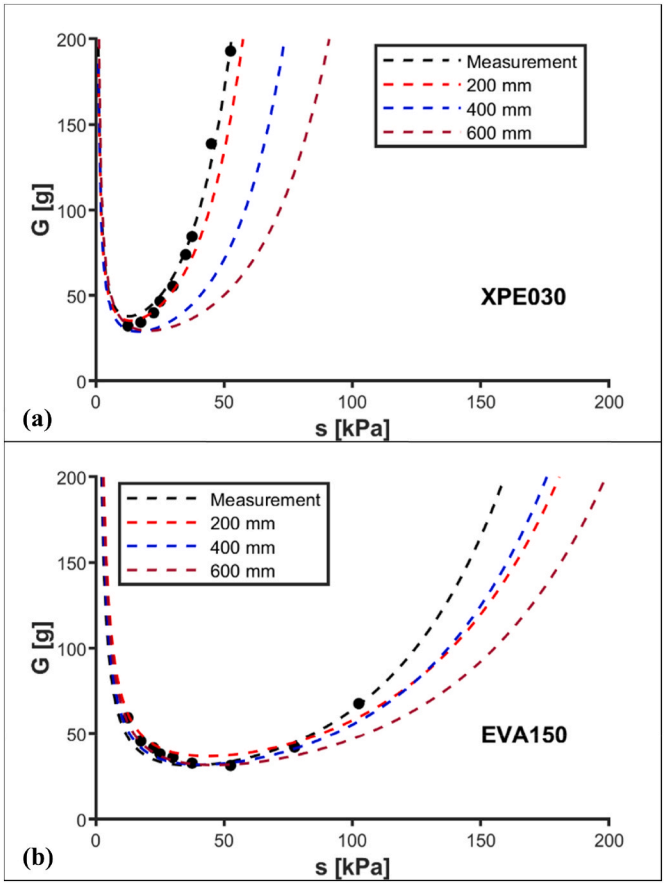

Fig. 8. Cushion curves of the 40 mm thick XPE030 (a) and EVA150 (b) foams measured with a drop height of 400 mm and calculated from data series of different drop heights.

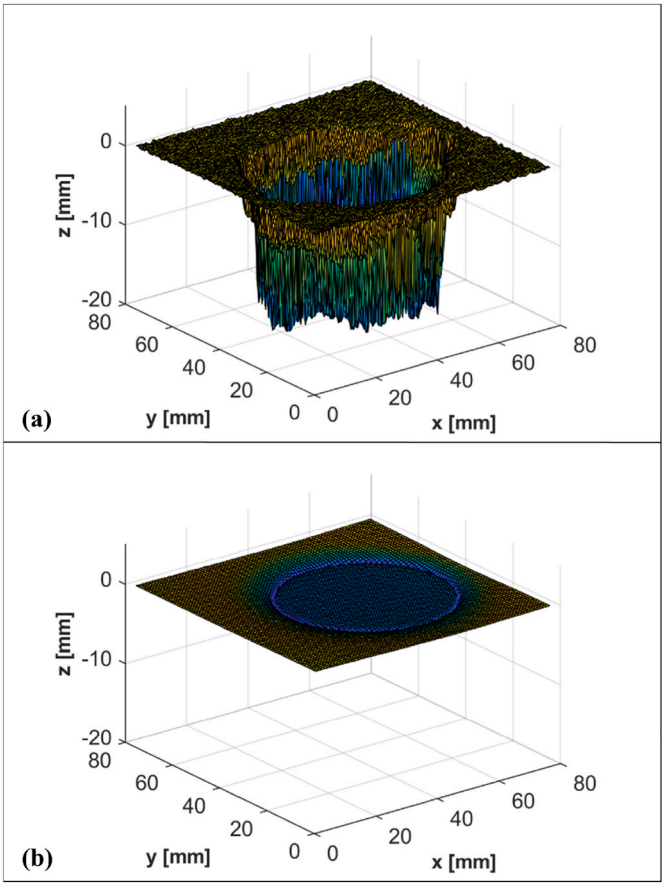

Fig. 9. 3D scanned image of the XPE030 (a) and EVA150 (b) samples showing the magnitude of irreversible deformation after impact testing at a static load of 103 kPa.

can be concluded that the calculation cannot take into account irreversible deformation, so the applicability of Burgess' method depends on the foam's resistance to the load.

As density increases, the range of static load where the calculation is still accurate widens, as the structural failure of a higher density foam requires higher impact energy. For EVA foams of increasing density (see Table 1), the upper static load limit for accurate prediction was approximately 30, 50, 70 and 100 kPa, while for XPE foams, this limit was around 20, 25, 30 and 45 kPa.

The 3D images of the impact-tested samples also validated our theory. The calculation gave the most inaccurate results for the XPE030 foam, as this sample proved to be the least resistant to impact loading (Fig. 9). In contrast, the EVA150 foam was the one where the calculated results can be used over the widest range of static load, as it suffered only minor permanent deformation even at 103 kPa.

The highest deformed volume appeared to be 28.3 cm^3 for the XPE030 sample, while in contrast, the least deformed EVA150 only showed 3.1 cm^3 of permanent deformation. The deformation of the other samples was between these two values and decreased in proportion to density. Increasing foam density can generally be assumed by smaller cells and thicker cell walls (see Section 2) usually result in higher foam density, which produces a higher stress plateau in the stress–strain curve [4]. Therefore, higher density foams absorb more energy until the start of the densification zone [4], which explains the smaller deformed volume in our case.

5. Conclusions

This study demonstrates a new approach to determining the cushion curves of polymeric foam packaging materials. We performed several drop test series on 30–70 kg/m^3 density cross-linked polyethylene and 50–150 kg/m^3 density ethylene-vinyl-acetate foams using increasing drop weights at three different drop heights. We investigated the relationship between peak force and the static load, and used it to define a general equation for cushion curves, which correctly describes material behavior outside the measurement range as well. The fitted equations demonstrated well the deformation response of the foam structures to increasing energy impacts, which explains the typical U shape of the curves. Then, we analyzed the effect of foam density and drop height on the constants describing the curves, using multiple linear regression and covariance analysis. Both approaches revealed the same differences between the impact behaviors of the two foam materials. The width of the safe static load range (C_2 constant), where the peak acceleration is low and the foam provides adequate protection, was affected by drop height and foam density regardless of foam type. In contrast, the dependence of coefficient C_1 on drop height and density, which mainly affects peak acceleration, differed for the two materials. As the microcellular EVA foams are more resistant to load, the magnitude of the peak force only depended on density, and the effect of drop height was negligible. However, both measurement height and foam density increased the peak values for the softer macrocellular XPE foams.

In the second part of the study, we investigated the limitations of using the approach of Burgess [23] for the calculation of the cushion curve. With this method, we can calculate the curves for any drop height and foam thickness based on the points of an already measured cushion curve. The comparison of the calculated and experimental data showed that the method only gives good agreement for lower static loads, and the limit of applicability highly depends on foam density. The 3D images of the tested samples proved that with increasing static loads and drop heights, the higher impact energy causes permanent deformation in the foam structure. We concluded that the calculation could not take into account the irreversible deformation, so the applicability of the method depends on the foam's resistance to the load.

Combining the results of the first and second parts of our study, we can now determine the cushion curves of XPE and EVA foams using Equation (9) and Table 3. With this method, we are able to calculate the cushion curves without any drop tests in the given static load range. In the past, the biggest drawback of the cushion curves was that it took hundreds of tests to calculate them. Now our study will allow the use of cushion curves to become more widespread in engineering applications.

Authors statement

Márton Tomin: Conceptualization, Methodology, Investigation, Validation, Formal analysis, Writing - Original Draft, Visualization, Supervision, Project administration. **Richárd Dominik Párizs:** Validation, Formal analysis, Writing - Review & Editing. **Márton Áron Lengyel:** Investigation, Validation, Writing - Original Draft. **Ákos Kmetty**: Conceptualization, Supervision, Writing - Review & Editing, Project administration.

Declaration of competing interest

The authors declare that they have no known competing financial interests or personal relationships that could have appeared to influence the work reported in this paper.

Data availability

The authors do not have permission to share data.

Acknowledgments

This research was supported by the Hungarian National Research, Development and Innovation Office (K 132462); The research reported in this paper is part of project no. BME-NVA-02, implemented with the support provided by the Ministry for Innovation and Technology of Hungary from the National Research, Development and Innovation Fund, financed under the TKP2021 funding scheme. Á. Kmetty is thankful for the support of János Bolyai Research Scholarship of the Hungarian Academy of Sciences and the support of ÚNKP-21-5 New National Excellence Program of the Ministry for Innovation and Technology from the source of the National Research, Development and Innovation Fund. M. Tomin thanks to the support of the ÚNKP-21-3 New National Excellence Program of the Ministry for Innovation and Technology from the source of the National Research, Development and Innovation Fund.

References

[1] C. Ge, Theory and practice of cushion curve: a supplementary discussion, Packag. Technol. Sci. 32 (2019) 185–197, https://doi.org/10.1002/pts.2427.
[2] T. Tábi, K. Pölöskei, The effect of processing parameters and calcium-stearate on the ejection process of injection molded poly(Lactic Acid) products, Period. Polytech. - Mech. Eng. 66 (2022) 17–25, https://doi.org/10.3311/PPme.18246.
[3] Z.X. Zhang, Y.M. Wang, Y. Zhao, X. Zhang, A.D. Phule, A new TPE-based foam material from EPDM/PPB blends, as a potential buffer energy-absorbing material, Express Polym. Lett. 15 (2021) 89–103, https://doi.org/10.3144/expresspolymlett.2021.10.
[4] M. Avalle, G. Belingardi, R. Montanini, Characterization of polymeric structural foams under compressive impact loading by means of energy-absorption diagram, Int. J. Impact Eng. 25 (2001) 455–472, https://doi.org/10.1016/S0734-743X(00)00060-9.
[5] M.A. Naeem, A. Gábora, T. Mankovits, Influence of the manufacturing parameters on the compressive properties of closed cell Aluminum foams, Period. Polytech. - Mech. Eng. 64 (2020) 172–178, https://doi.org/10.3311/PPme.16195.
[6] Yu Zhong, Zhao Zhu, Zhang Phule, Influence of different ratio of CO2/N2 and foaming additives on supercritical foaming of expanded thermoplastic polyurethane, Express Polym. Lett. 16 (2022) 318–336, https://doi.org/10.3144/expresspolymlett.2022.24.
[7] N. Mills, Polymer Foams Handbook: Engineering and Biomechanics Applications and Design Guide, Elsevier Science, Oxford, 2007.
[8] D. Eaves, Handbook of Polymer Foams, Rapra Technology, Shawbury, UK, 2004.
[9] N.M. Mills, Polyolefin Foams, Rapra Technology Limited, Shawbury, 2003.
[10] K. Brown, Package Design Engineering, Wiley, New York, 1959.
[11] N.J. Mills, C. Fitzgerald, A. Gilchrist, R. Verdejo, Polymer foams for personal protection: cushions, shoes and helmets, Compos. Sci. Technol. 63 (2003) 2389–2400, https://doi.org/10.1016/S0266-3538(03)00272-0.
[12] H. Zhao, Testing of polymeric foams at high and medium strain rates, Polym. Test. 16 (1997) 507–516, https://doi.org/10.1016/S0142-9418(97)00012-3.
[13] Y. Guo, J. Zhang, Shock absorbing characteristics and vibration transmissibility of honeycomb paperboard, Shock Vib. 11 (2004), 936804, https://doi.org/10.1155/2004/936804.
[14] Y. Guo, W. Xu, Y. Fu, H. Wang, Dynamic shock cushioning characteristics and vibration transmissibility of X-PLY corrugated paperboard, Shock Vib. 18 (2011), 578265, https://doi.org/10.3233/SAV-2010-0559.
[15] A. Joodaky, G.S. Batt, J.M. Gibert, Prediction of cushion curves of polymer foams using a nonlinear distributed parameter model, Packag. Technol. Sci. 33 (2020) 3–14, https://doi.org/10.1002/pts.2473.
[16] P.J. Marcon, T.J.K. Strang, C.C. Institute, Cushion Design Using the CCI Cushion Design Calculator and PadCAD, Canadian Conservation Institute, Ottawa, 1994.
[17] A. Miliner, Package Designer Software Manual, Software Version 2.0, CDO Technologies, 2013.
[18] American Society for Testing and Materials, Standard Test Method for Dynamic Shock Cushioning Characteristics of Packaging Material, ASTM D1596-14, 2014. https://www.astm.org/d1596-14r21.html. Number of pages: 4.
[19] G. Gruenbaum, J. Miltz, Static versus dynamic evaluation of cushioning properties of plastic foams, J. Appl. Polym. Sci. 28 (1983) 135–143, https://doi.org/10.1002/app.1983.070280112.
[20] J. Miltz, G. Gruenbaum, Evaluation of cushioning properties of plastic foams from compressive measurements, Polym. Eng. Sci. 21 (1981) 1010–1014, https://doi.org/10.1002/pen.760211505.
[21] O. Ramon, J. Miltz, Prediction of dynamic properties of plastic foams from constant–strain rate measurements, J. Appl. Polym. Sci. 40 (1990) 1683–1692, https://doi.org/10.1002/app.1990.070400922.
[22] M.A. Sek, M. Minett, V. Rouillard, B. Bruscella, A new method for the determination of cushion curves, Packag. Technol. Sci. 13 (2000) 249–255, https://doi.org/10.1002/pts.517.
[23] G. Burgess, Consolidation of cushion curves, Packag. Technol. Sci. 3 (1990) 189–194, https://doi.org/10.1002/pts.2770030403.
[24] G. Burgess, Generation of cushion curves from one shock pulse, Packag. Technol. Sci. 7 (1994) 169–173, https://doi.org/10.1002/pts.2770070403.
[25] M. Tomin, Á. Kmetty, Polymer foams as advanced energy absorbing materials for sports applications—a review, J. Appl. Polym. Sci. 139 (2022), 51714, https://doi.org/10.1002/app.51714.
[26] M. Tomin, Á. Kmetty, Evaluating the cell structure-impact damping relation of cross-linked polyethylene foams by falling weight impact tests, J. Appl. Polym. Sci. 138 (2021), 49999, https://doi.org/10.1002/app.49999.
[27] A. Kmetty, M. Tomin, T. Barany, T. Czigany, Static and dynamic mechanical characterization of cross-linked polyethylene foams: the effect of density, Express Polym. Lett. 14 (2020) 503–509, https://doi.org/10.3144/expresspolymlett.2020.40.
[28] G. Wang, J. Zhao, G. Wang, L.H. Mark, C.B. Park, G. Zhao, Low-density and structure-tunable microcellular PMMA foams with improved thermal-insulation and compressive mechanical properties, Eur. Polym. J. 95 (2017) 382–393, https://doi.org/10.1016/j.eurpolymj.2017.08.025.
[29] G. Wang, G. Zhao, G. Dong, Y. Mu, C.B. Park, Lightweight and strong microcellular injection molded PP/talc nanocomposite, Compos. Sci. Technol. 168 (2018) 38–46, https://doi.org/10.1016/j.compscitech.2018.09.009.
[30] X. Sun, H. Kharbas, J. Peng, L.-S. Turng, A novel method of producing lightweight microcellular injection molded parts with improved ductility and toughness, Polymer 56 (2015) 102–110, https://doi.org/10.1016/j.polymer.2014.09.066.